Induction Shimming

Daniel Wollmann

25th August 2009

Acknowledgments

- A. Bernhard, S. Ehlers, G. Fuchert, A.-S. Müller, P. Peiffer, T. Baumbach, LAS, University of Karlsruhe
- S. Casalbuoni, A. Grau, M. Hagelstein, D. Saez de Jauregui, U. Retzlaff (†), R. Rossmanith, ISS/ANKA, FZK
- E. Mashkina, B. Kostka, M. Weißer, M. Magerl, E. Steffens, University of Erlangen-Nürnberg

Special thanks:

- D. Erbe, ISS, FZK
- R. Semerad, W. Prusseit, THEVA GmbH, Ismanning
- C. Boffo, M. Borlein, Babcock Noell GmbH, Würzburg

Outline

Introduction - Synchrotron Radiation

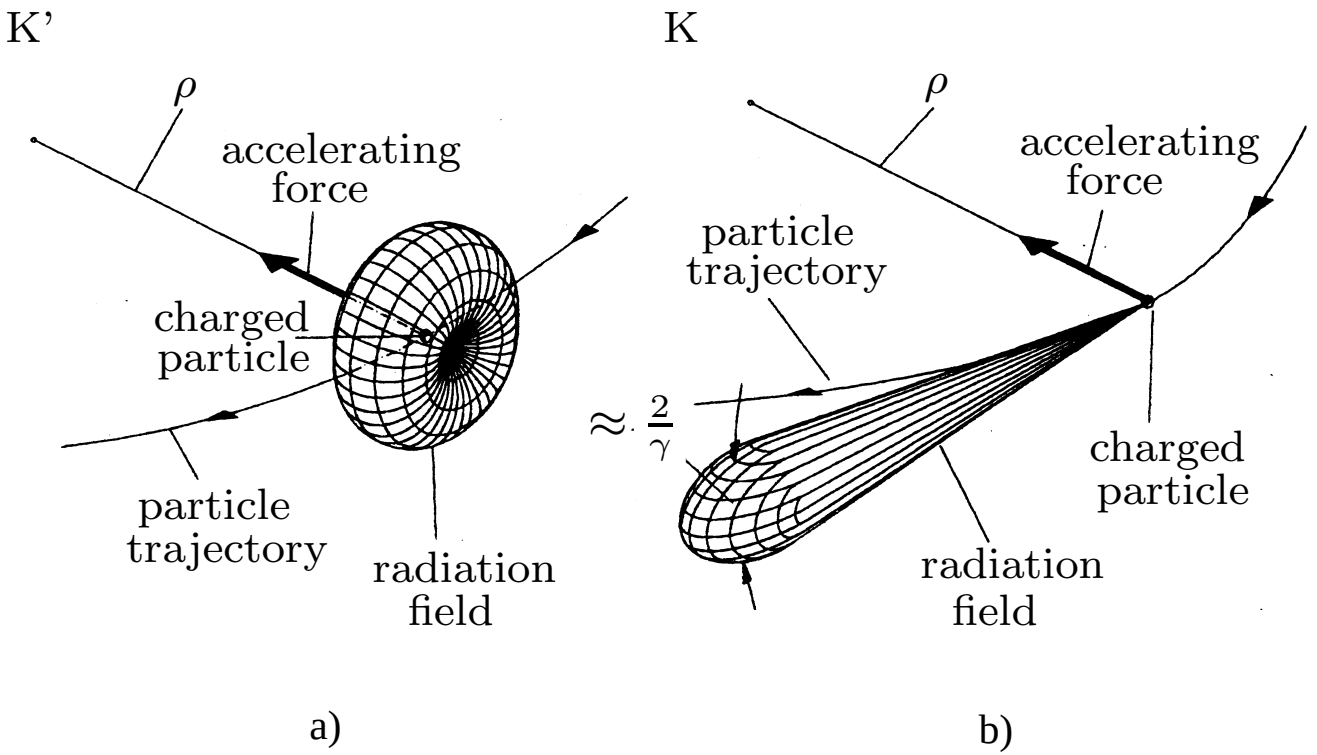

after K. Wille: *Physik der Teilchenbeschleuniger*

- Power: $P_\gamma \propto \frac{E^4}{\rho^2}$
- White spectrum (from the far infrared to hard X-rays)

Introduction - Synchrotron Radiation Sources

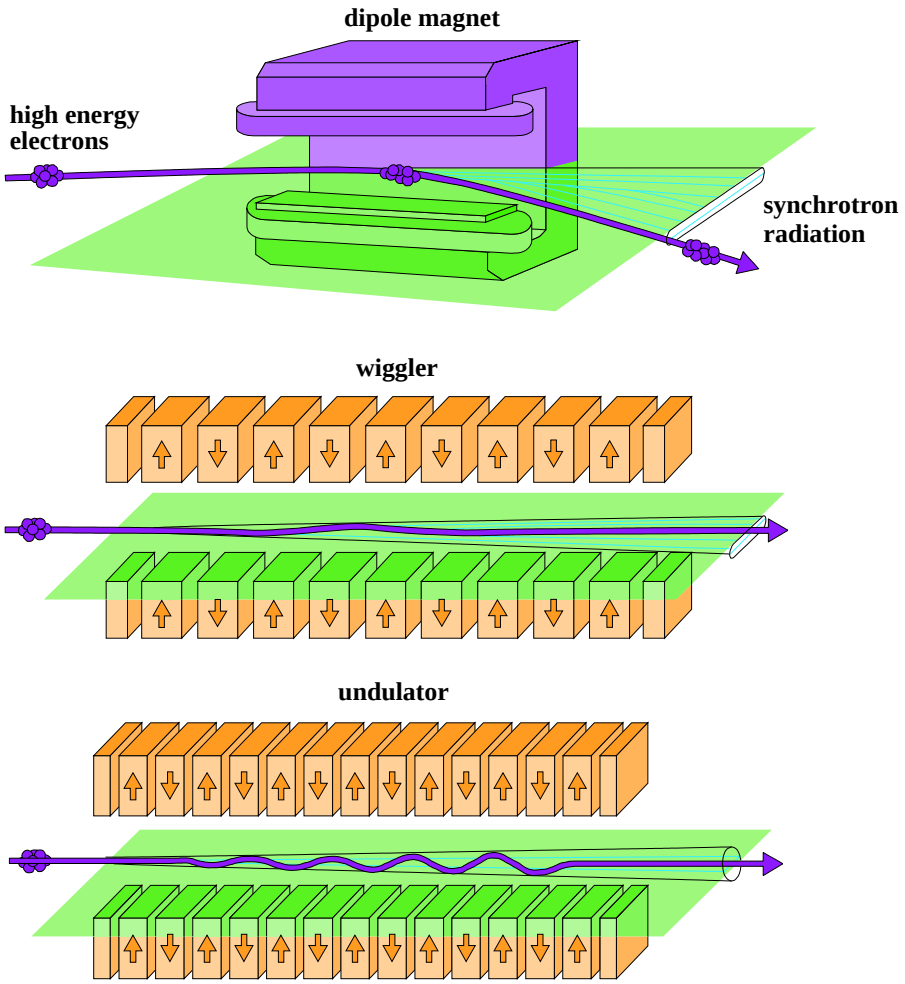

Courtesy ESRF

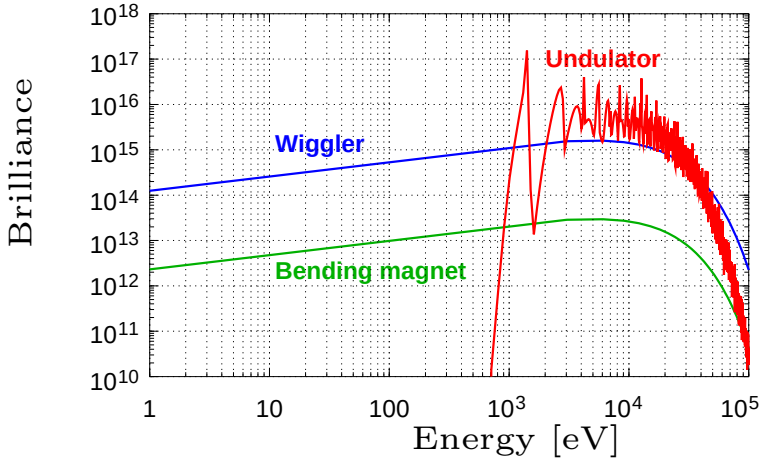

Courtesy R. Butzbach

Introduction - Superconductive Undulators

Structure of a superconductive undulator (Vectorfields Opera3D)

Undulator equation:

$$\lambda_L = \frac{\lambda_u}{2k\gamma^2}\left(1 + \frac{K^2}{2} + \Theta^2\gamma^2\right)$$

with

$K = 0.0934 \cdot \lambda_u[mm] \cdot \tilde{B}[T]$.

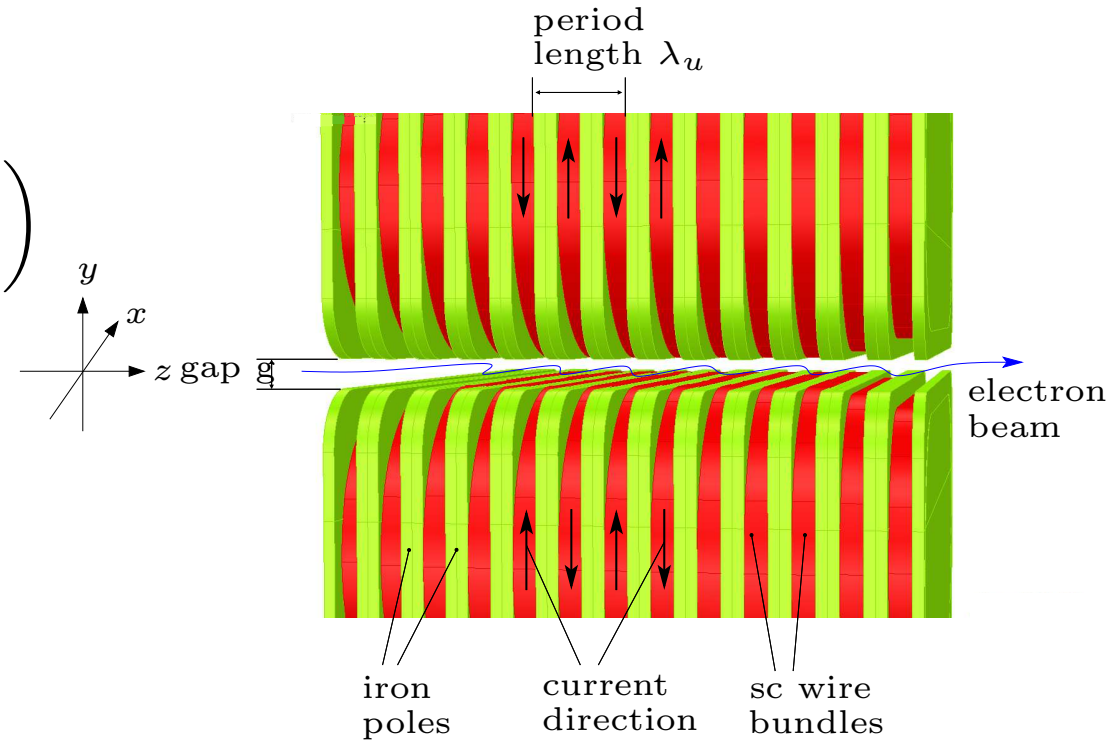

Introduction - Undulators - Phase Requirements

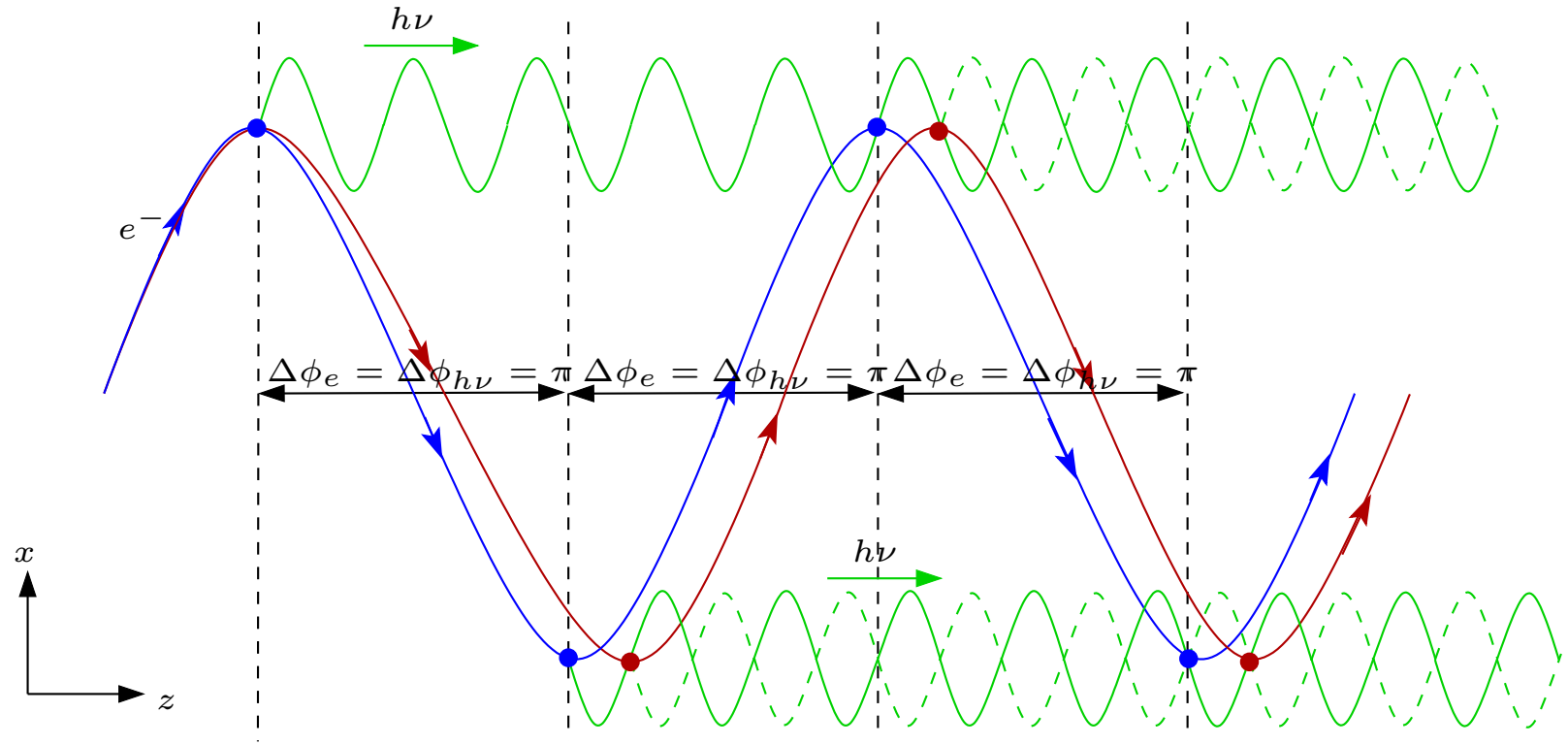

$$\Phi_{error} = \sqrt{\frac{\sum_{i=1}^{2n} (\tilde{\Phi}_i)^2}{2n}}$$

Introduction - Undulators - Spectra

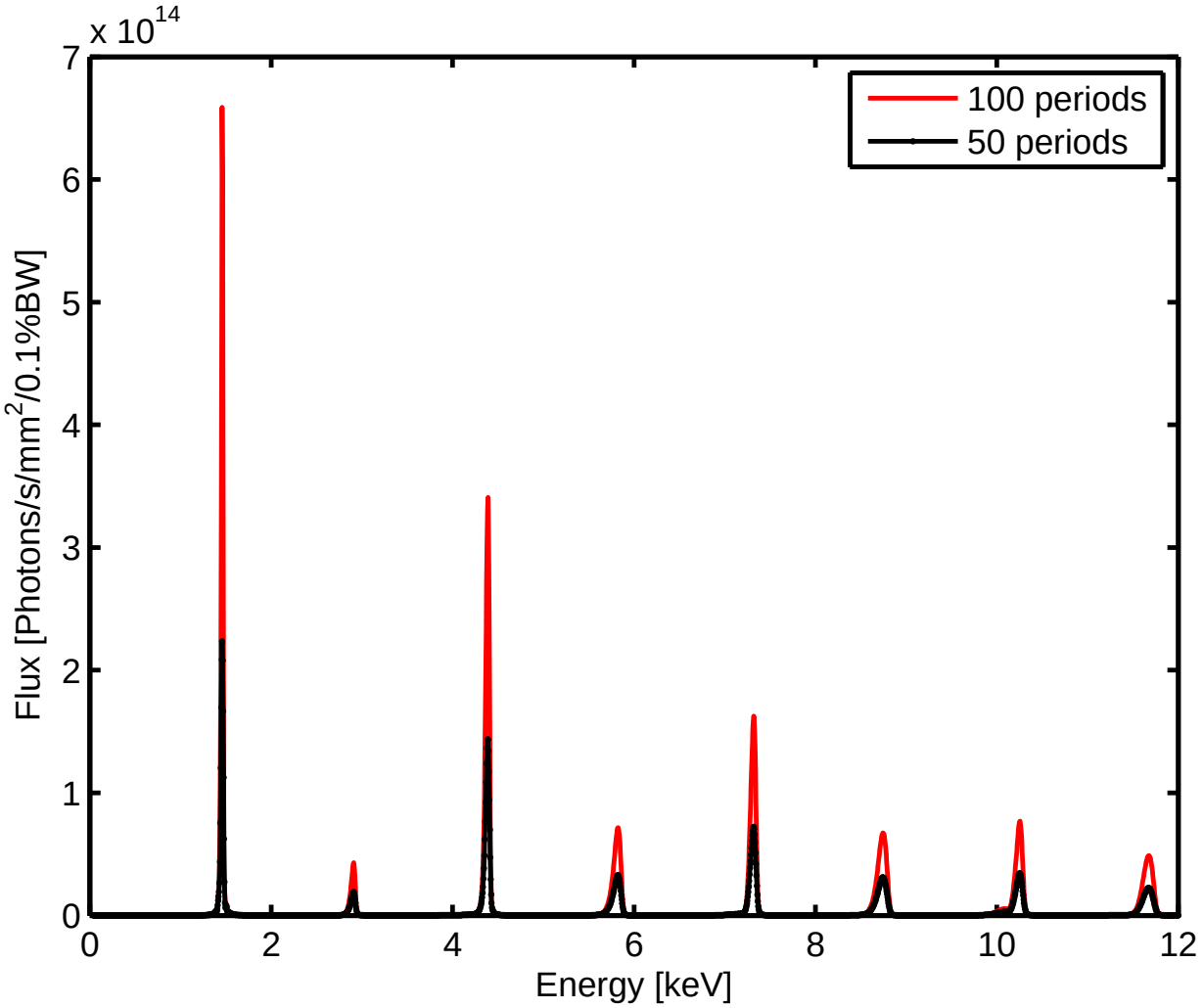

Introduction - Mechanical Deviations

- Variation of the pole position
- Variation of the wire-bundle position
- Variation of the period-length

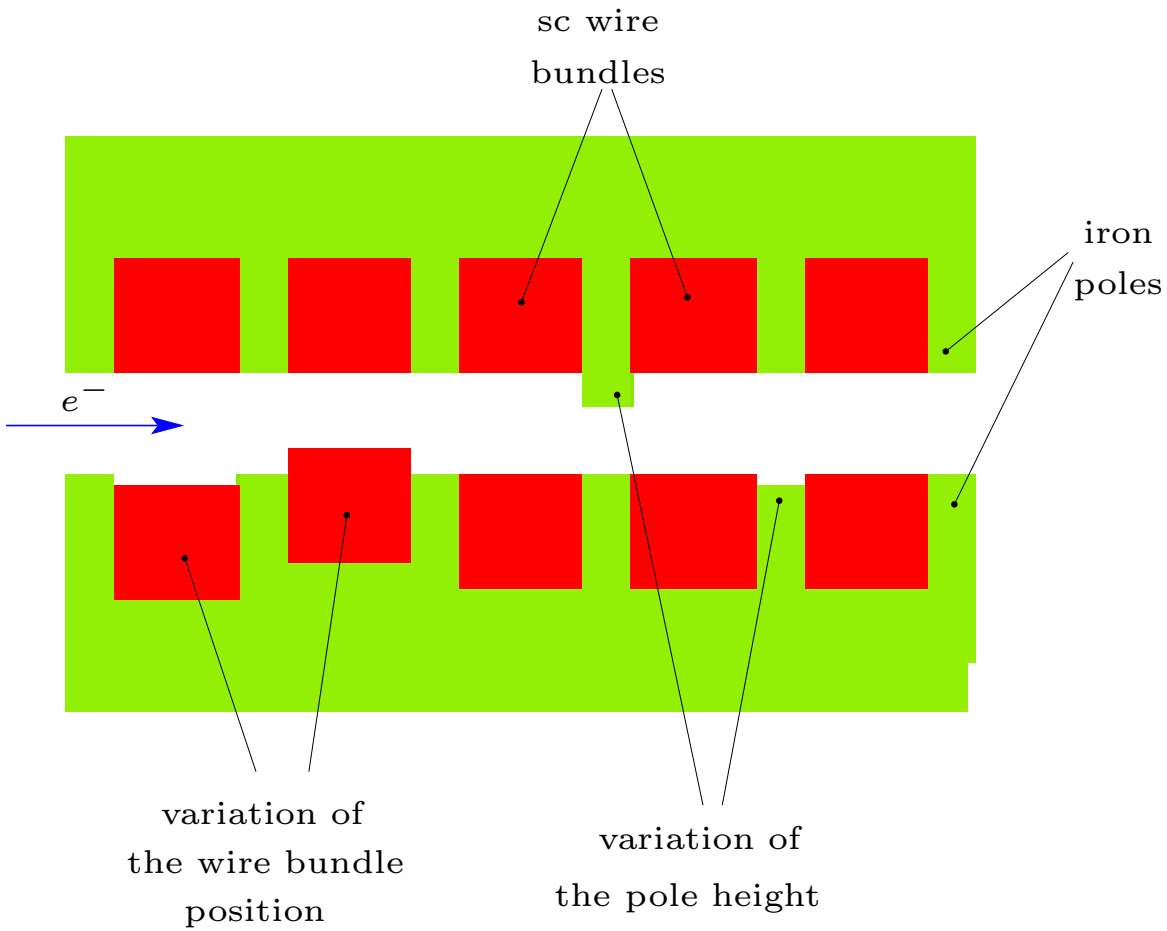

Induction-Shimming: Faraday's law of induction

$$\oint_C \tilde{\mathbf{E}} d\vec{l} = -\frac{d}{dt} \int_S \tilde{\mathbf{B}} d\vec{A},$$

- $\tilde{\mathbf{B}}$ is the magnetic flux density over the area S with the contour C
- $\tilde{\mathbf{E}}$ is the electrical field strength
- $d\vec{A}$ is the surface element

Using a superconductive closed-loop along the contour C, yields

$$0 = \frac{d}{dt} \int_S \tilde{\mathbf{B}} d\vec{A}.$$

Induction-Shimming: Rectangular fields, one closed-loop

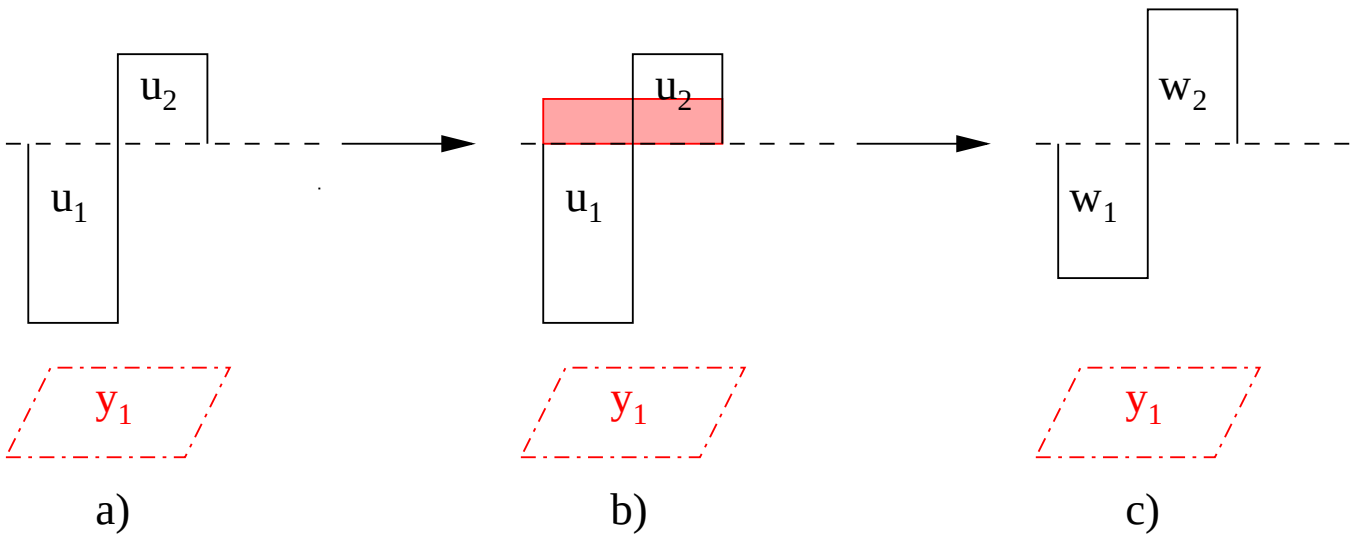

a) b) c)

$$y_1 + u_1 + u_2 = 0 \qquad (1)$$

$$w_1 = u_1 + \frac{1}{2}y_1 \qquad (2)$$

$$w_2 = u_2 + \frac{1}{2}y_1 \qquad (3)$$

$$\rightarrow w_2 = -w_1 = w \qquad (4)$$

$$w = -u_1 - \frac{1}{2}y_1$$

$$w = u_2 + \frac{1}{2}y_1$$

$$\rightarrow w = \frac{-u_1 + u_2}{2} \qquad (5)$$

Induction-Shimming: Rectangular fields, two closed-loops

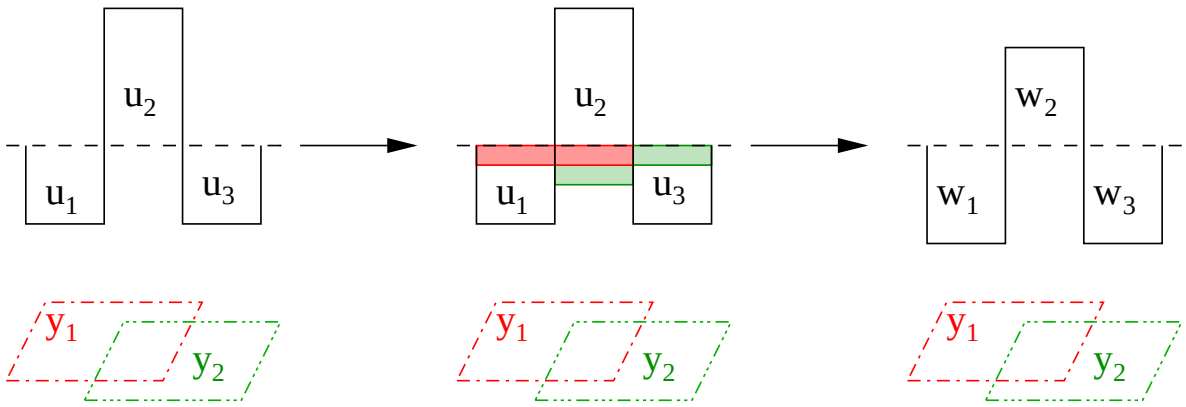

a) b) c)

$$y_1 + u_1 + u_2 + \frac{1}{2}y_2 = 0 \quad (6)$$

$$y_2 + u_2 + u_3 + \frac{1}{2}y_1 = 0 \quad (7)$$

$$w_1 = u_1 + \frac{1}{2}y_1 \quad (8) \qquad w = -u_1 - \frac{1}{2}y_1$$

$$w_2 = u_2 + \frac{1}{2}y_1 + \frac{1}{2}y_2 \quad (9) \qquad w = u_2 + \frac{1}{2}y_1 + \frac{1}{2}y_2$$

$$w_3 = u_3 + \frac{1}{2}y_2 \quad (10) \qquad w = -u_3 - \frac{1}{2}y_2$$

$$\rightarrow w_2 = -w_1 = -w_3 = w \quad (11) \qquad \rightarrow w = \frac{-u_1 + u_2 - u_3}{3} \quad (12)$$

Induction-Shimming: Rectangular fields, n closed-loops

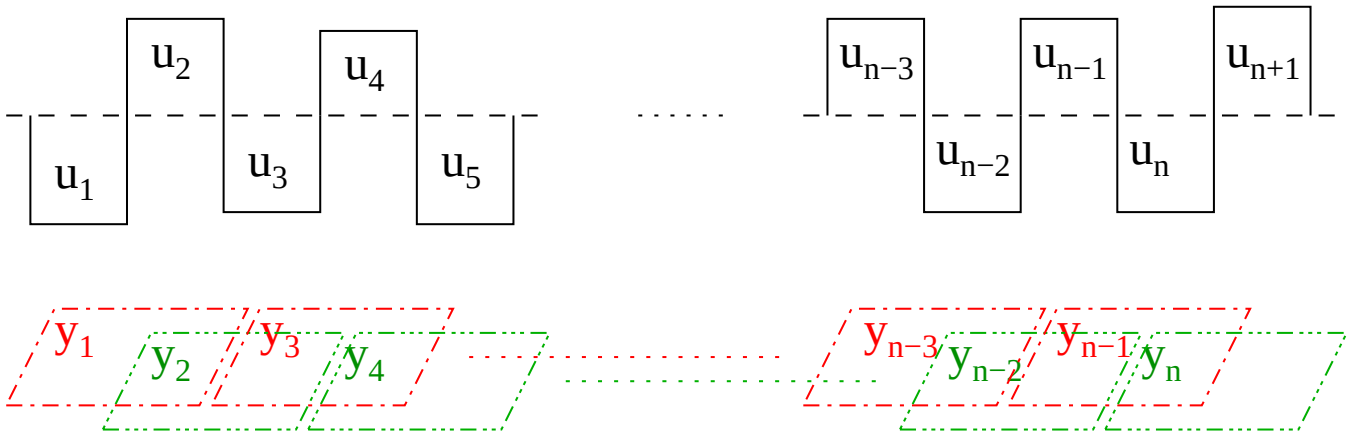

$$w = \frac{\pm u_1 \mp u_2 \pm \ldots \pm u_n \mp u_{n+1}}{n+1} \tag{13}$$

Induction-Shimming: Biot-Savart Model

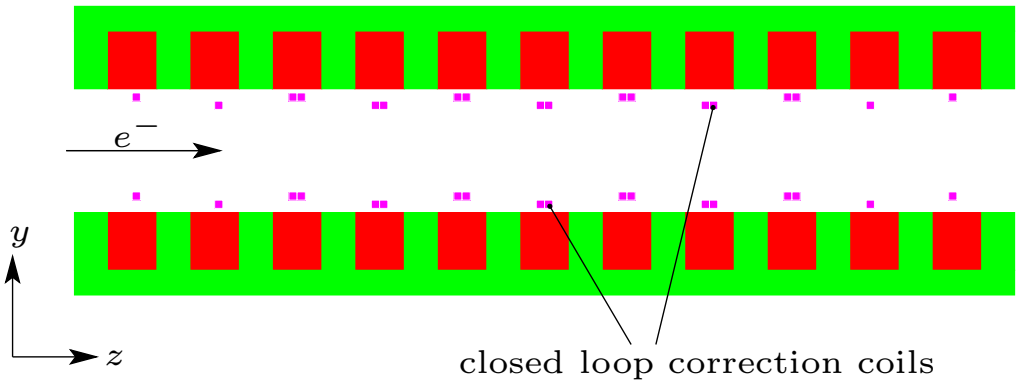

Faraday's law of induction for one closed-loop:

$$\dot{I}_i = -\frac{1}{L}\dot{\Phi}_i. \qquad (14)$$

The coupling between loop i and loop j with a mutual inductance M_{ij}:

$$\dot{I}_i = M_{ij}\dot{I}_j. \qquad (15)$$

Combining equation (14) and (15), solving for $\dot{\Phi}$:

$$\dot{\Phi}_i = L\left(\sum_{j\neq i} M_{ij}\dot{I}_j - \dot{I}_i\right) \qquad (16)$$

The self-inductance L and the mutual inductances M_{ij} are defined by the geometrical arrangement and the design of the closed-loops.

Induction-Shimming: Biot-Savart Model

Integration of equation (16) yields

$$\begin{pmatrix} \Phi_1 \\ \Phi_2 \\ \\ \vdots \\ \Phi_{2N-1} \end{pmatrix} = -M_{cc} \cdot \begin{pmatrix} I_1 \\ I_2 \\ \\ \vdots \\ I_{2N-1} \end{pmatrix}, \tag{17}$$

with the symmetrical matrix

$$M_{cc} = \begin{pmatrix} L & a_1 & a_2 & \cdots & a_{2N-1} \\ a_1 & & & \ddots & \vdots \\ a_2 & & \ddots & & a_2 \\ \vdots & \ddots & & & a_1 \\ a_{2N-1} & \cdots & a_2 & a_1 & L \end{pmatrix}, \tag{18}$$

with $a_k = L \cdot M_{i,j}$ and $k = |j - i|$.

Measurements - Setup

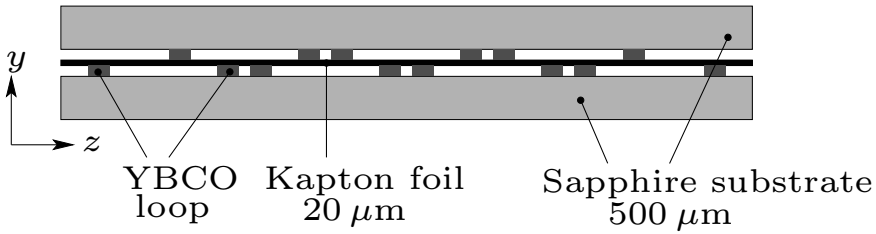

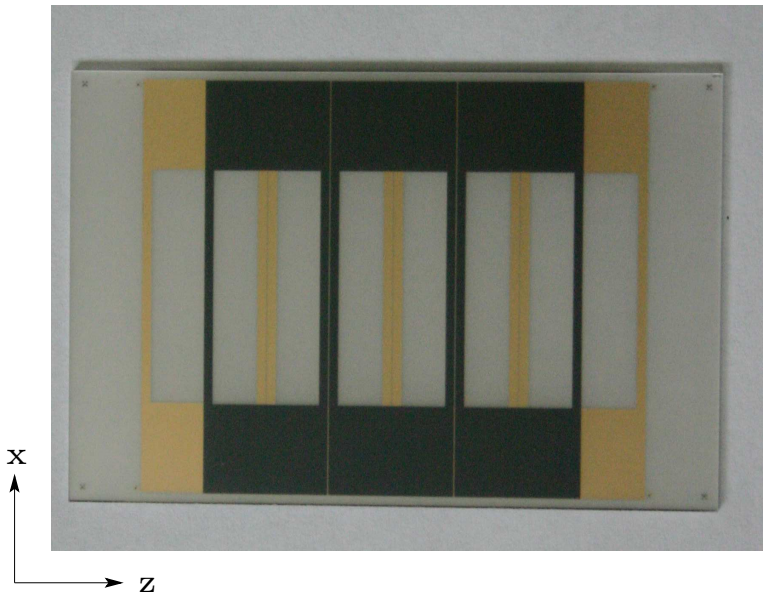

- 330 nm thick YBCO loops on a 500 μm sapphire substrate
- YBCO structures are covered by 200 nm thick gold layer
- dimensions (z-x-plane): $14 \times 44\,\mathrm{mm}^2$
- two structures (4 loops, 3 loops) stacked, results in a system of 7 overlapping closed-loops
- mounted in a frame on the surface of a mock-up coil
- measured in the cryostat CASPER at FZK with Hall-probe slide

Measurements - Setup

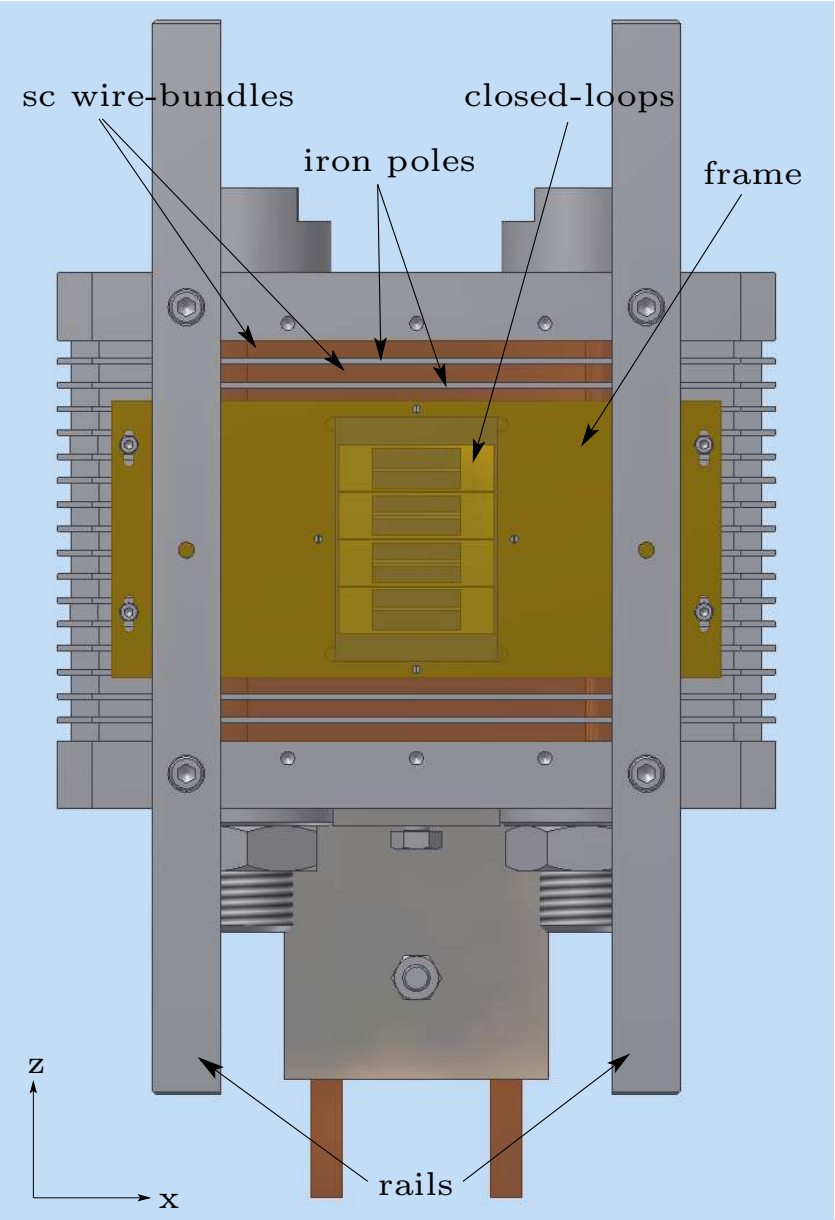

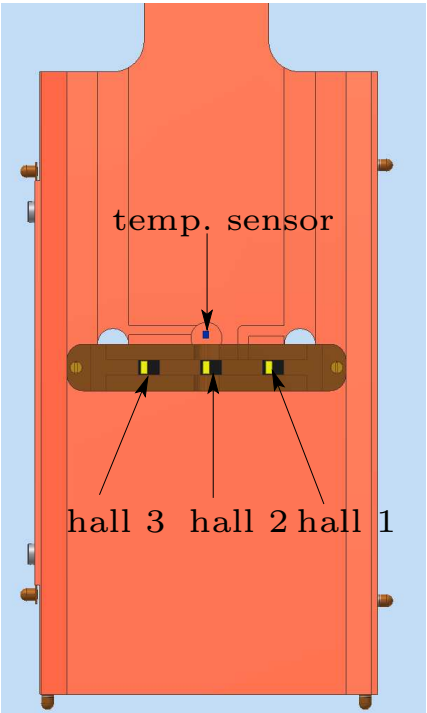

Measurements - Setup

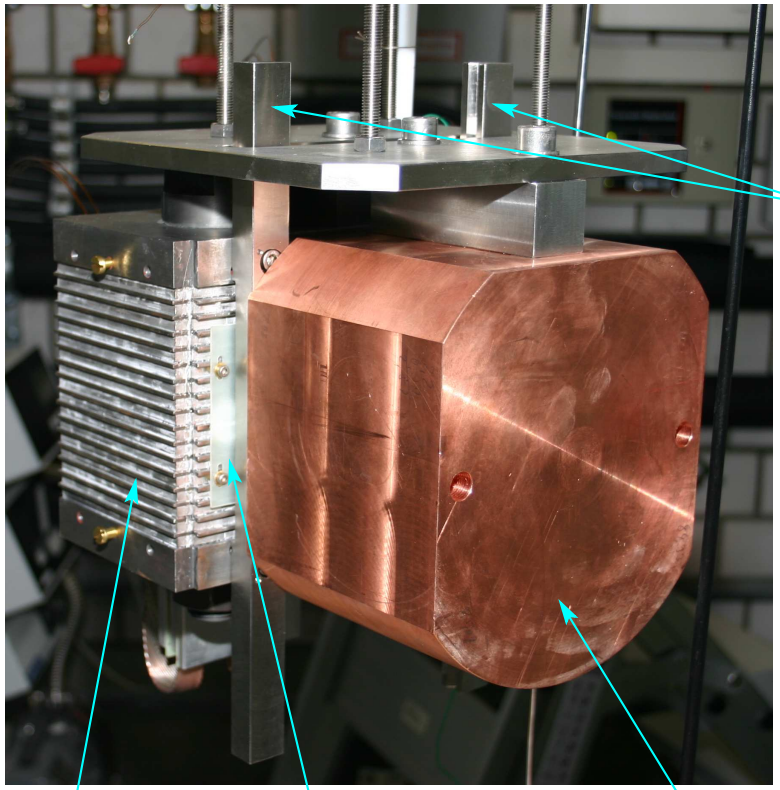

Field at 350A without Induction-Shimming

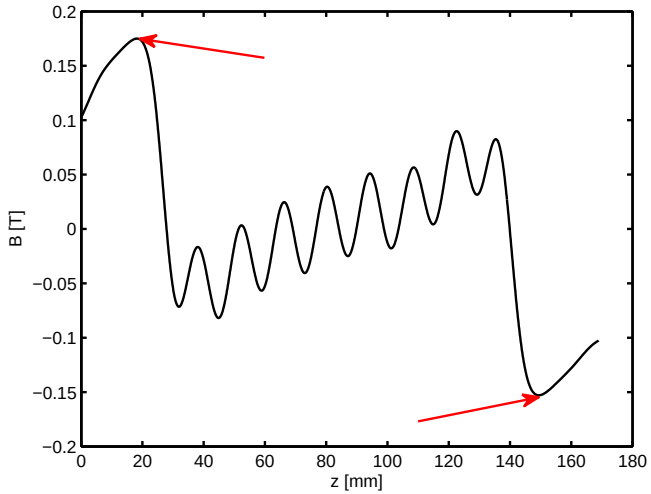

Measurements - Results (70 A)

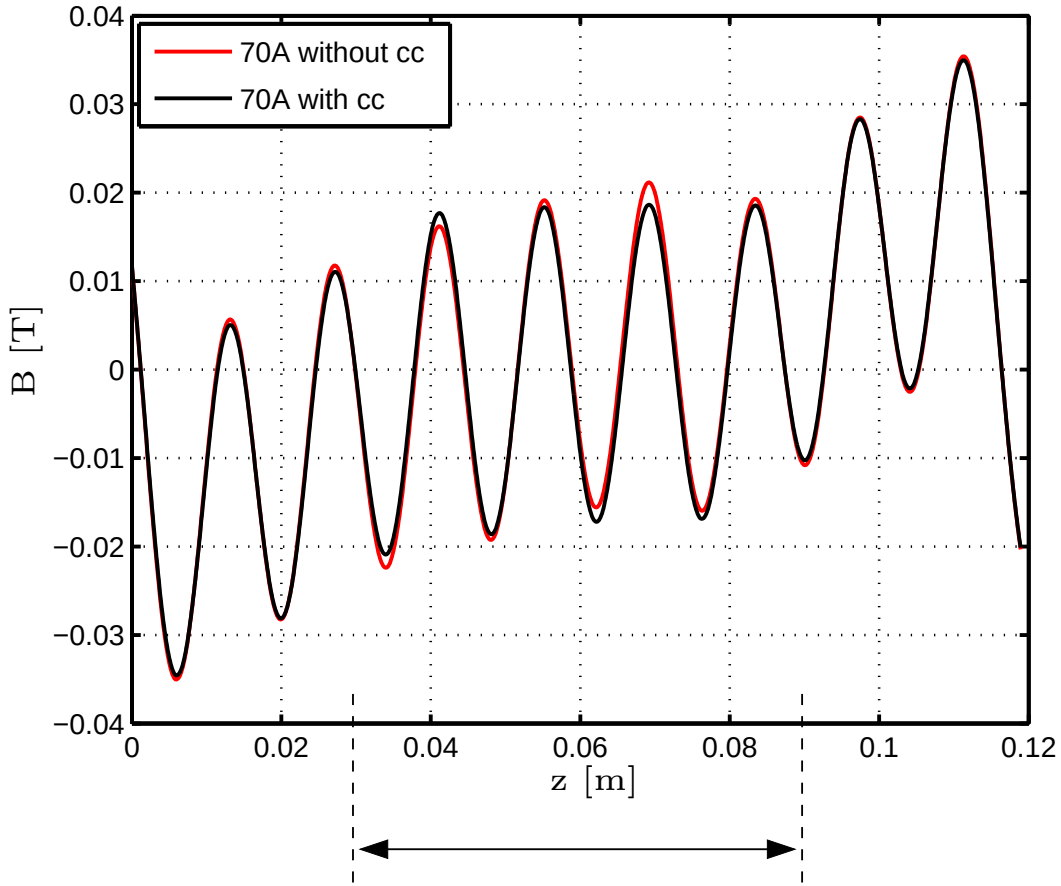

closed-loop system

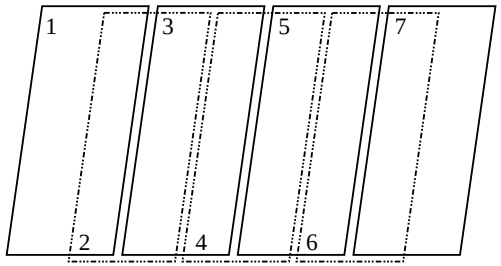

Measurements - Results (70 A)

Field comparison

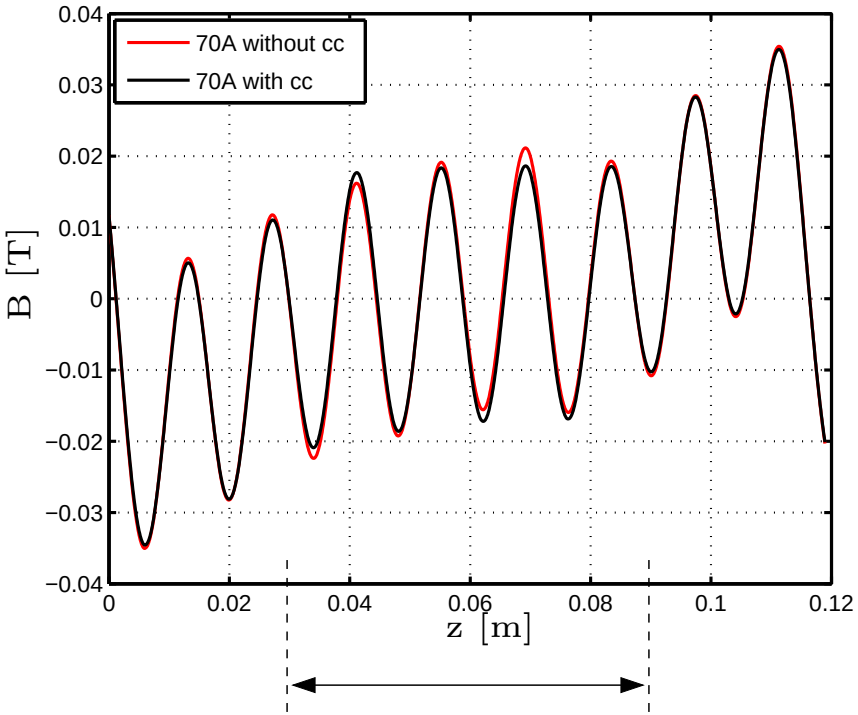

closed-loop system

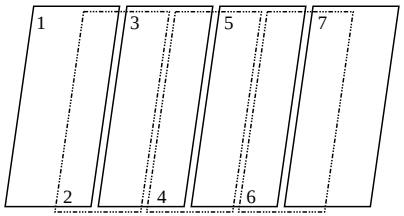

Difference field

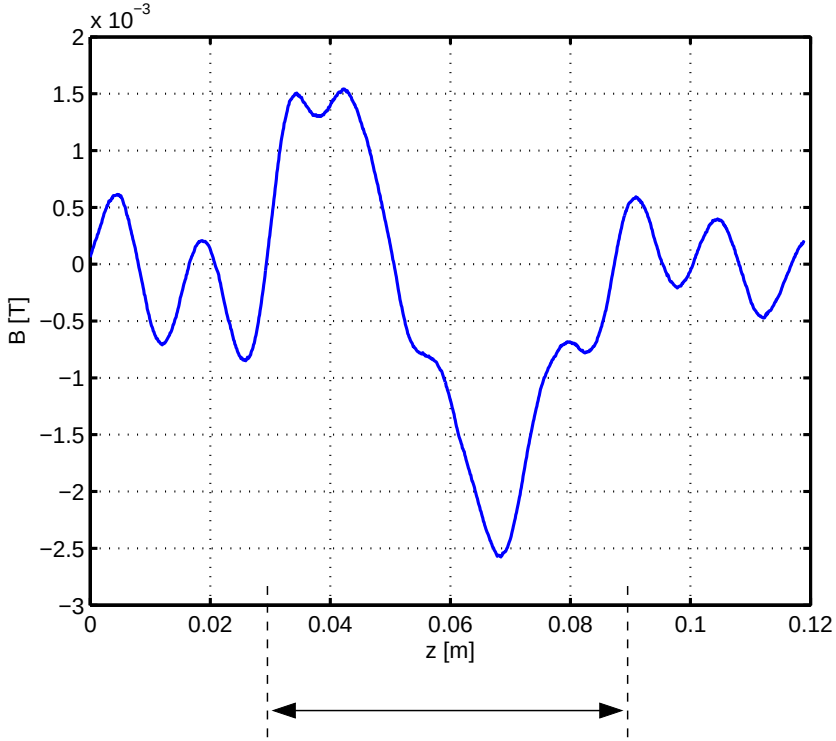

closed−loop system

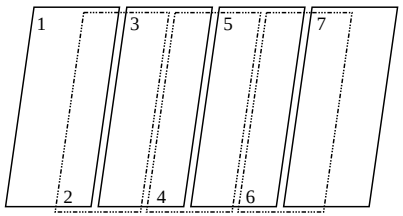

Measurements - Results (70 A)

Diff. field & Biot-Savart model

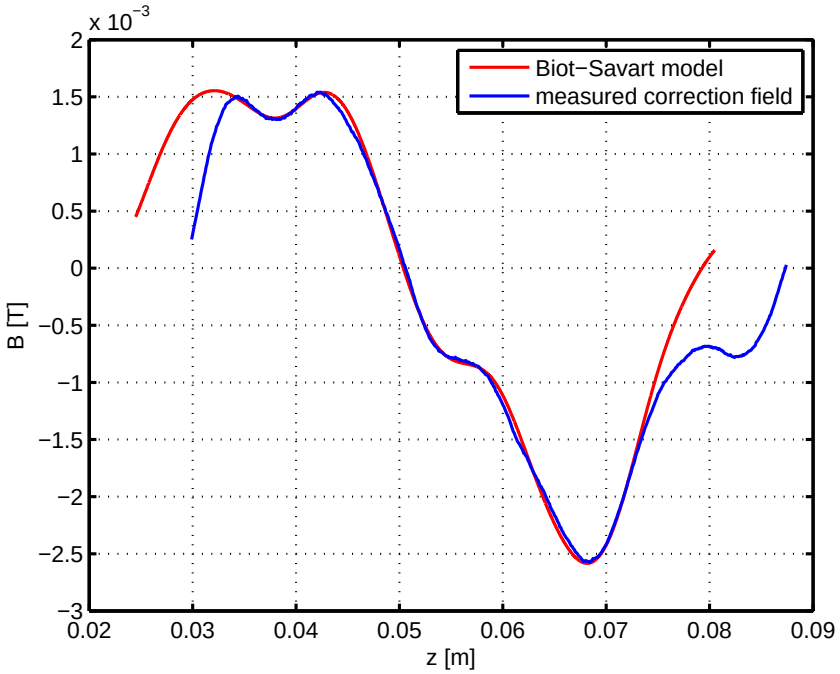

Phase difference

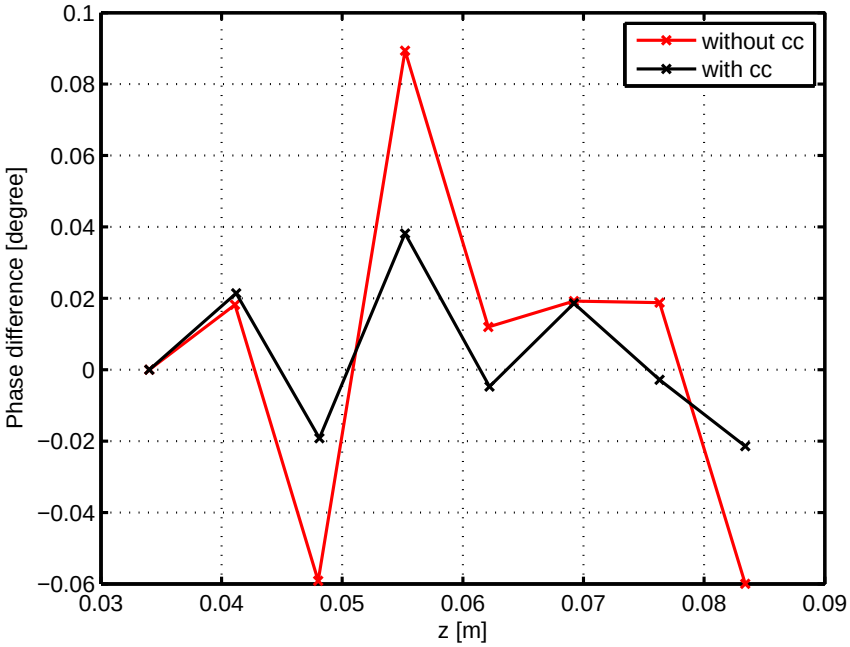

Correction currents induced into the loops:

	loop 1	loop 2	loop 3	loop 4	loop 5	loop 6	loop 7
current [A]	56	-2.0	61	-51.5	13.5	-86	-23

Measurements - Results (70 A)

First field integral I_1

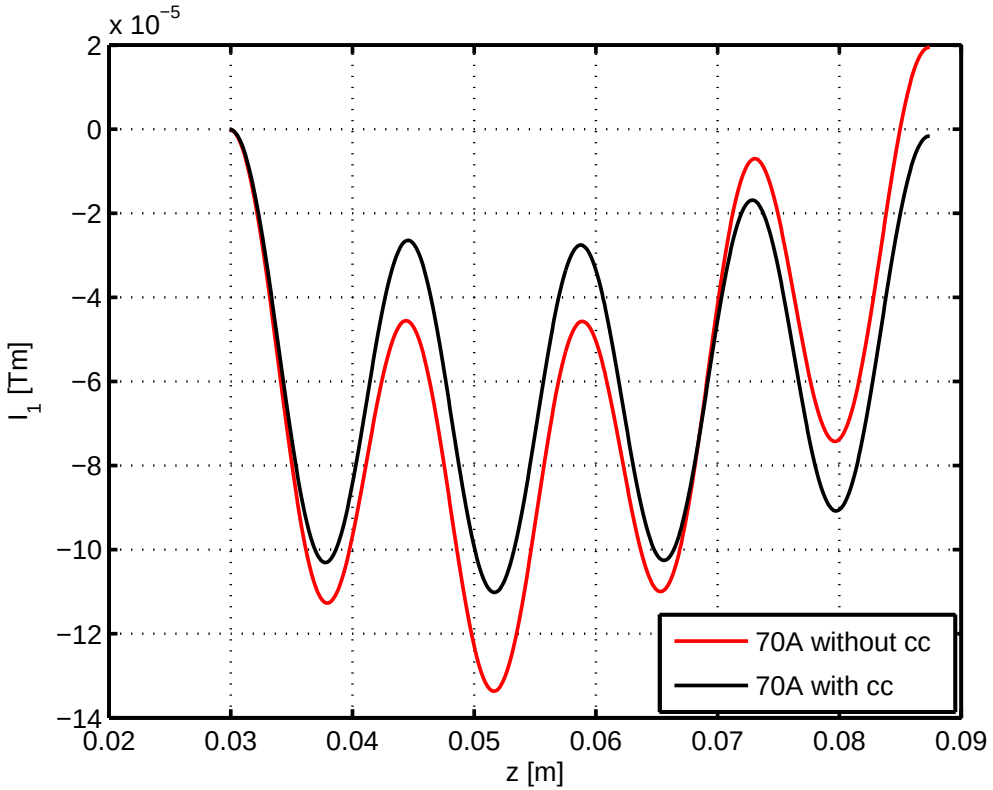

- local reduction of I_1
  $\longrightarrow$ reduction of phase error
- no global reduction of I_1

Measurements - Results

Change of correction field pattern from lower to higher currents I_{main}

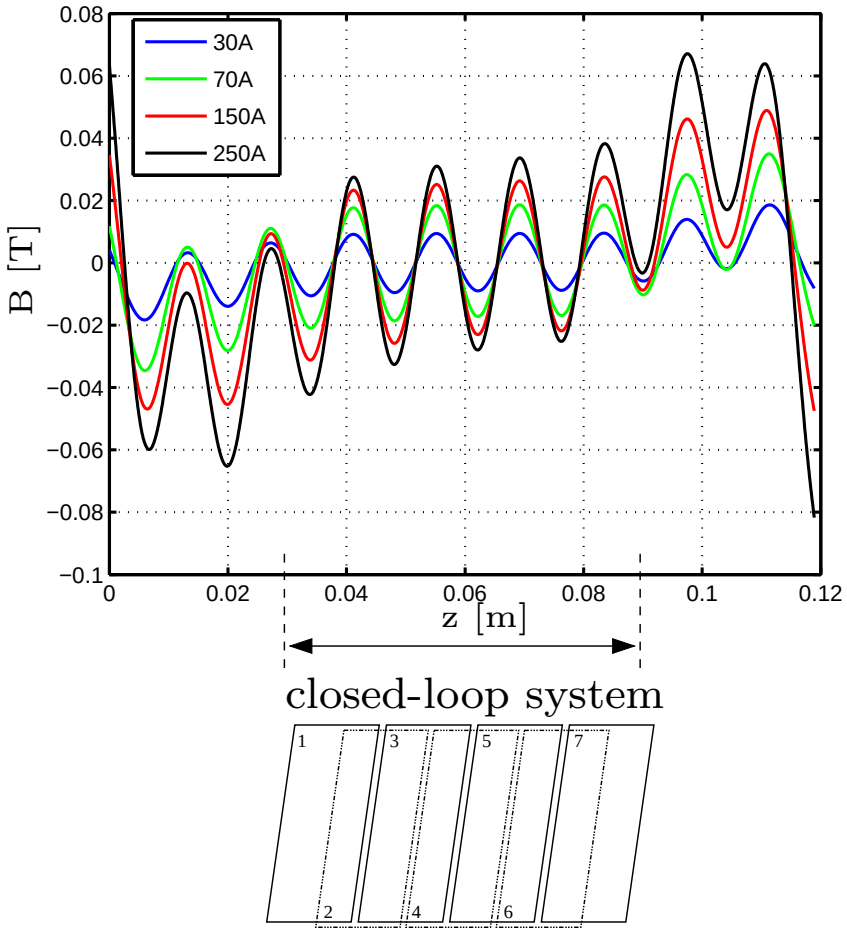

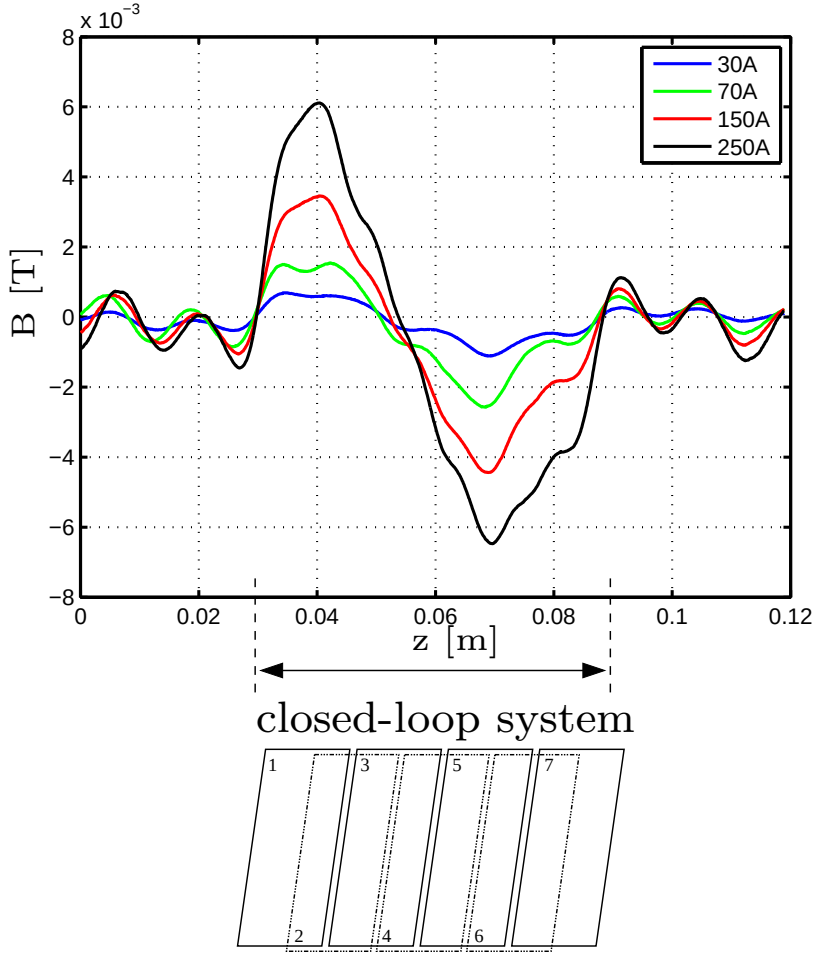

Measurements - Results

Variation of adjacent extrema

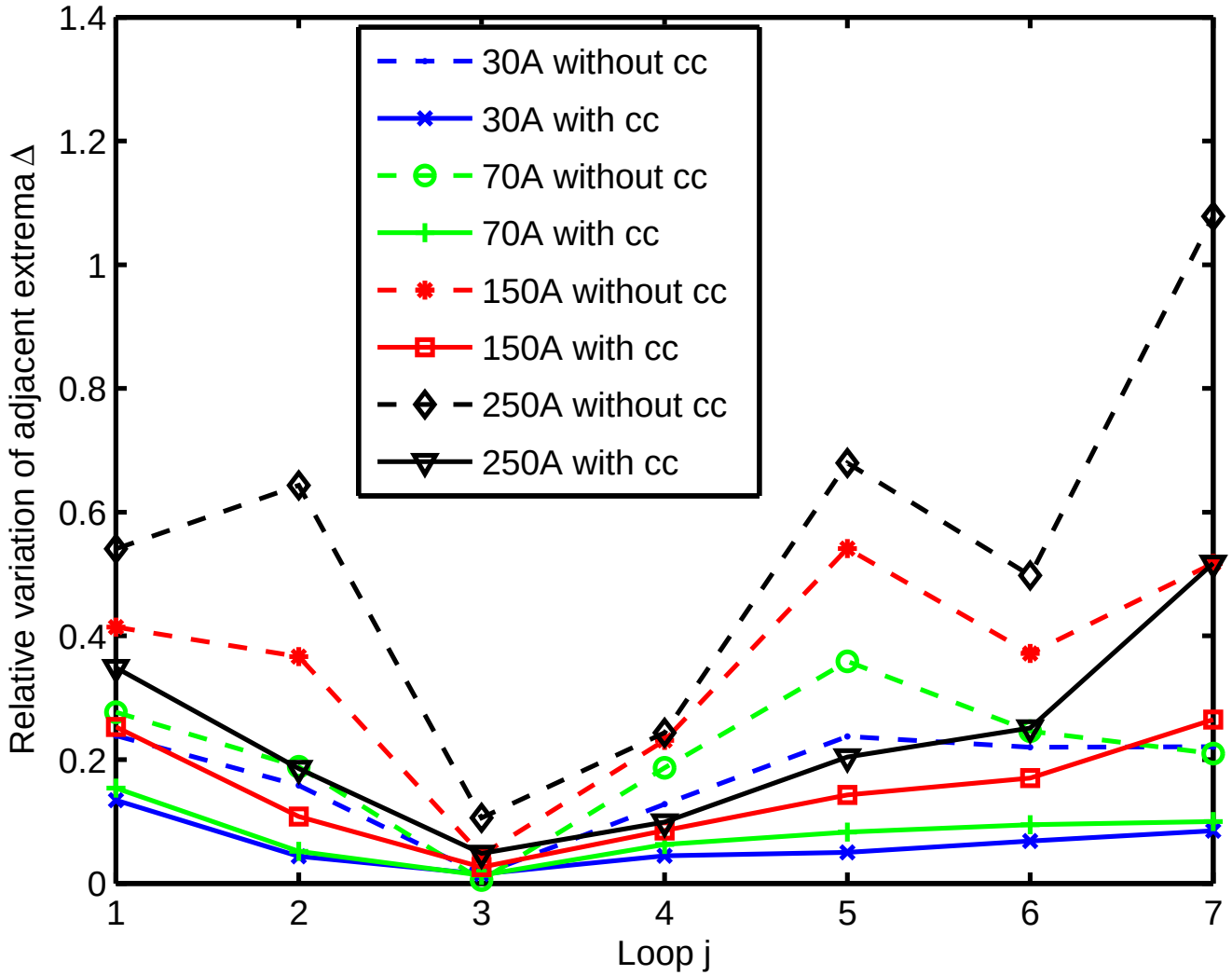

Measurements - Results

Hysteretic behaviour after $I_{main} = 250\,\mathrm{A}$

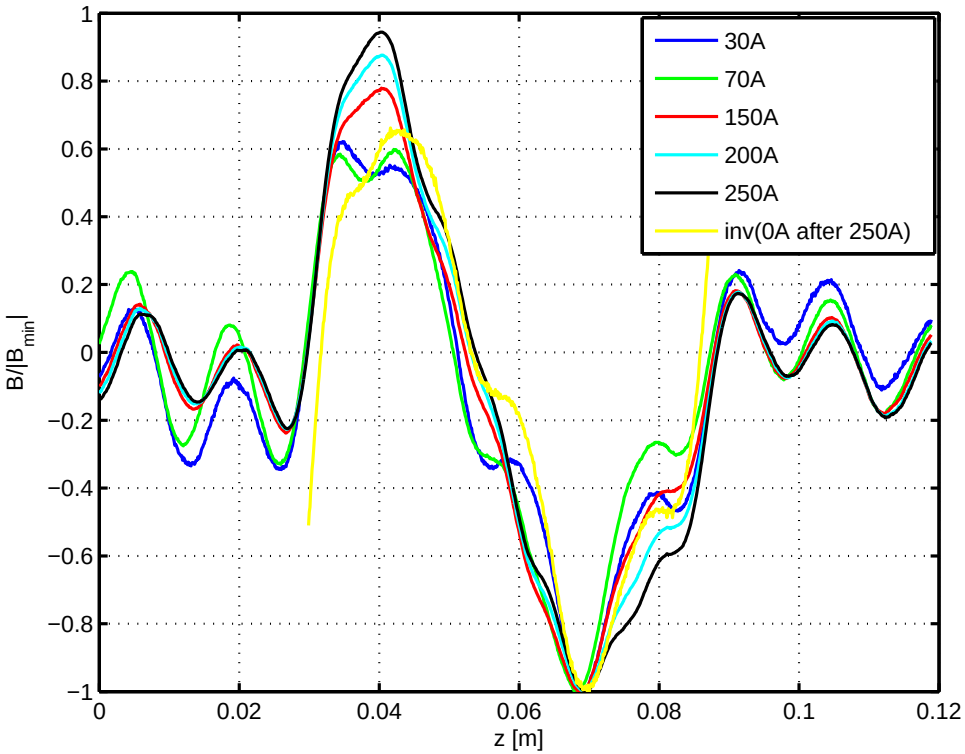

Possible reasons:

1. eddy currents around vortices in the type-II superconductor
2. critical current density reached in parts of the loop system

- shape of residual field (yellow) implies second

Measurements - Results

Current in mock-up coil	Induced currents in closed-loop [A]						
	1	2	3	4	5	6	7
30 A	22.8	1.3	21.5	-25.8	8.4	-39.5	-7
50 A	43	-1.0	47	-39	15.7	-63.2	-13
70 A	56	-2.0	61	-51.5	13.5	-86	-23
100 A	45	34	49.5	-29	-10	-92.5	-46
150 A	54	67	66.5	-20.5	-23	-111	-76
200 A	62	102	81	-20.7	-40	-119.5	-110.5
250 A	60	150	75	-25.8	-50	-160	-110
0 A after 250 A	-3	-4.5	-6.7	6.3	-3.5	14.3	4.5

Conclusion - Results and Challenges

- Induction-shimming is an field error dependent passive correction scheme
- Theoretically described by Faraday's law of induction
- Experimentally proven with a 7 closed-loop test device
- Correction fields up to 10% of main field measured
- Correction does not fail when critical current in YBCO is exceeded

→ Test with a complete undulator (12 period short prototype currently under construction) and two 12 loop induction-shimming devices (already available)

→ Reduction of substrate thickness

→ Longer induction-shimming systems (from 15 up to 100 periods)

→ tbd if required field quality for damping wigglers can be achieved with the help of induction-shimming